JOURNAL OF GEOPHYSICAL RESEARCH, VOL. 103, NO. D1, PAGES 1607-1618, JANUARY 20, 1998

Interhemispheric asymmetry in the 1 mbar O_3 trend: An analysis using an interactive zonal mean model and UARS data

D. B. Considine,[1,2] A. E. Dessler,[1,2] C. H. Jackman,[2] J. E. Rosenfield,[2,3] P. E. Meade,[2,4] M. R. Schoeberl,[2] A. E. Roche,[5] and J. W. Waters[6]

Abstract. Trends in O_3 calculated from solar backscattered ultraviolet (SBUV) observations near 1 mbar are more negative at high latitudes in the southern hemisphere than in the northern hemisphere [*Hood et al.*, 1993]. A mechanism is presented that produces an interhemispheric O_3 trend asymmetry similar to the observed asymmetry in the Goddard Space Flight Center dynamically interactive zonal mean model. Upper Atmosphere Research Satellite (UARS) data are then examined for evidence that the atmospheric trend asymmetry is produced by a similar mechanism. The model O_3 trend asymmetry is mainly due to interhemispheric differences in odd chlorine (Cl_y) partitioning. The asymmetry in Cl_y partitioning is caused primarily by lower amounts of CH_4 and NO in the southern hemisphere than the northern hemisphere high latitudes, due to differences in the dynamical behavior of the model hemispheres. Symmetric increases in Cl_y are accompanied by a southern hemisphere increase in ClO that is larger than in the northern hemisphere. Concentrations of CH_4 and N_2O retrieved by the cryogenic limb array etalon spectrometer aboard UARS during 1992 are lower in the southern hemisphere fall and winter seasons at high latitudes in the upper stratosphere than in the northern hemisphere, favoring higher southern hemisphere ClO values. However, observations of ClO by the microwave limb sounder on UARS do not show consistently higher values in the southern hemisphere compared with the northern hemisphere in 1992, 1993, or 1994. The UARS data therefore do not confirm that a mechanism similar to the model mechanism occurs in the real atmosphere and is the cause of the SBUV O_3 trend asymmetry.

1. Introduction

Long-term satellite observations of atmospheric O_3 concentrations indicate that the amount of O_3 in the middle and upper stratosphere has decreased over the past 15 years. Decreases in O_3 similar to the observations are predicted by global two-dimensional models of stratospheric photochemistry to be a consequence of increased amounts of stratospheric chlorine [*World Meteorological Organization WMO*, 1995]. The similarity between the model predictions and the satellite-observed trends is a crucial link in the theory connecting anthropogenic chlorine emissions to stratospheric O_3 depletion. It is therefore important to examine and determine the cause of any discrepancies between the model predictions and observations.

One feature of the O_3 trends calculated from solar backscattered ultraviolet (SBUV) and SBUV 2 data is a substantially more negative trend at high southern latitudes than high northern latitudes. A recent analysis of Stratospheric Aerosol and Gas Experiment (SAGE) and SAGE II satellite data shows a similar asymmetry [*Wang et al.*, 1996]. This asymmetry is not replicated in model O_3 trend calculations, which typically have similar magnitudes in the northern and southern hemispheres.

The SBUV trend asymmetry is shown in Figure 1a which is a plot of the annually averaged trend in percent per year calculated using both SBUV and SBUV 2 data. The combined data set extends from November 1978 through June 1994 [*Hollandsworth et al.*, 1995], although SBUV 2 provides no data in winter poleward of 60° or poleward of 40° after 1992. The southern hemisphere trend is about 40% larger in magnitude than the

[1]Joint Center for Earth System Science, University of Maryland, College Park.

[2]NASA Goddard Space Flight Center, Greenbelt, Maryland.

[3]General Sciences Corporation, Laurel, Maryland.

[4]Applied Research Corporation, Landover, Maryland.

[5]Lockheed Palo Alto Research Laboratories, Palo Alto, California.

[6]Jet Propulsion Laboratory, Pasadena, California.

Paper number 97JD02363.
0148-0227/98/97JD-02363$09.00

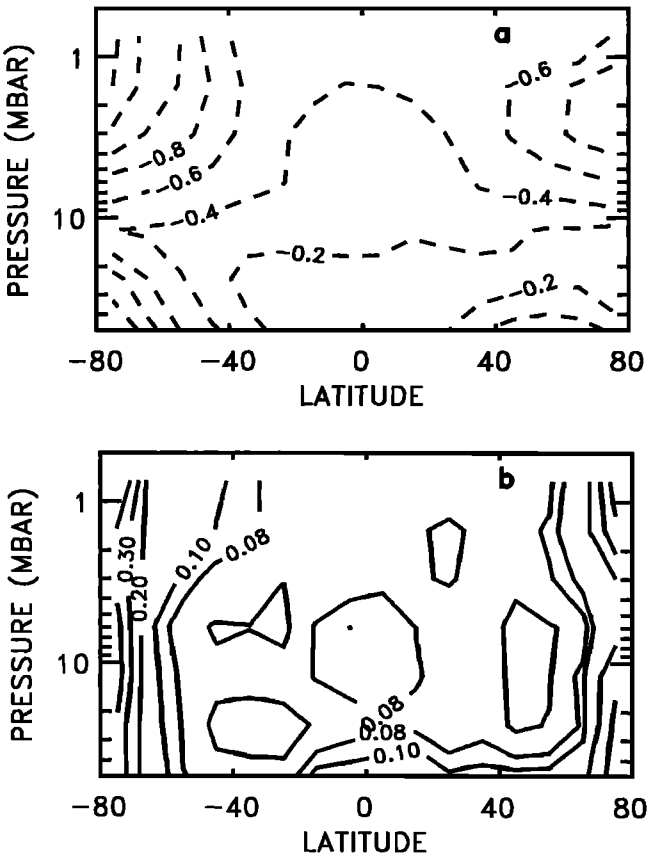

Figure 1. (a) Annually averaged trend in O_3 calculated from the combined Nimbus 7 solar backscattered ultraviolet (SBUV) and Nimbus 11 SBUV 2 instrument data sets, in percent per year. (b) Statistical error (1σ) in the annually averaged trend calculated from the combined SBUV and SBUV 2 instruments.

northern hemisphere trend, peaking above 1.4% compared with about 1 %/yr. The 1σ precision uncertainty of this result is shown in Figure 1b. The difference between the southern and northern hemisphere high-latitude trends around 1 mbar is similar in magnitude to the 1σ uncertainty, suggesting that the difference is real. The statistical significance of the asymmetry is marginal, however, and it is also possible but somewhat unlikely that the asymmetry is due to uncertainties in the trend calculation. No mechanism has yet been suggested to explain the asymmetric loss of O_3. Determining its cause is complicated because few observations of other atmospheric constituents that might establish the cause of the trend asymmetry were taken during the time that the changes in O_3 occurred. Instruments on UARS have made observations of many important stratospheric trace constituents since its launch in late 1991, and data from UARS may provide some clues.

The Goddard Space Flight Center (GSFC) operates two zonal mean models of stratospheric photochemistry and dynamics. One is designed as an assessment tool and is driven by a residual circulation that is calculated off-line from observations [*Douglass et al.*, 1989; *Jackman et al.*, 1990; *Considine et al.*, 1994]. The second model is primarily a research tool and calculates its residual circulation interactively using model-calculated O_3 and a planetary wave dissipation parameterization forced by topography [*Bacmeister et al.*, 1995; *Rosenfield et al.*, 1997]. The O_3 trend of each of these models is shown in Figures 2a and 2b. The trend is calculated as the annually averaged percent change in O_3 between two model runs to steady state using 1980 and 1990 boundary conditions. The boundary value fluxes used in these runs were taken from *WMO* [1990, Table 3.2].

The trend calculated with the assessment model is typical of other zonal mean model trend calculations and shows little interhemispheric asymmetry [e.g., *WMO*, 1995]. The interactive model, on the other hand, exhibits a large asymmetry. Although the southern hemisphere trend peak occurs in the model between 5 and 10 mbar instead of at 1 mbar as observed, the model calculated trend is qualitatively similar to the observations, with the southern hemisphere peak trend about 50% larger than the northern hemisphere peak trend.

The major difference between these two models is the model dynamics. In the interactive model, interhemispheric topographical differences force a southern hemisphere residual circulation characterized by much less meridional mixing due to planetary wave activity

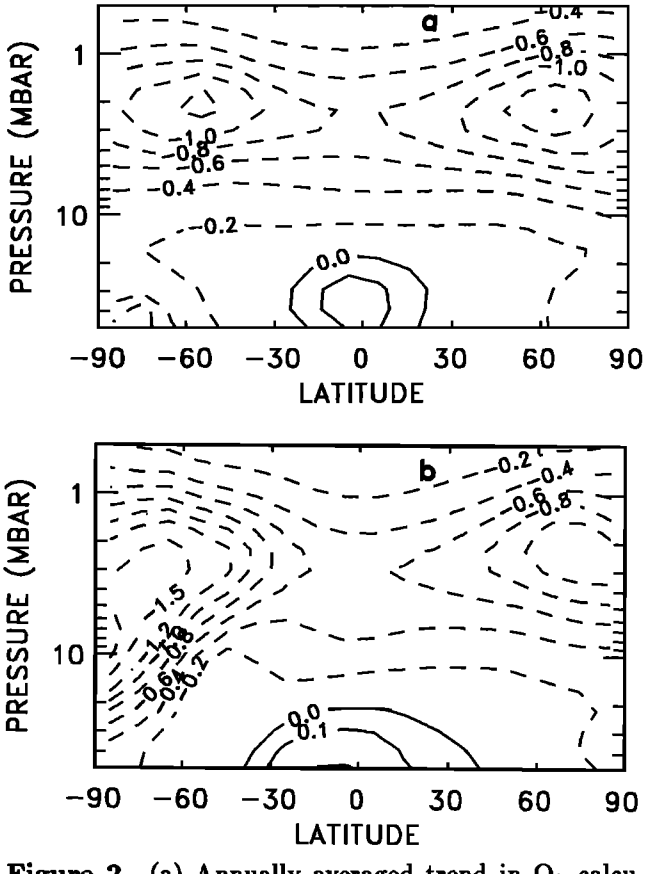

Figure 2. (a) Annually averaged trend in O_3 calculated by the Goddard Space Flight Center (GSFC) assessment model, in percent per year. (b) Annually averaged trend in O_3 calculated by the GSFC interactive model, in percent per year.

and a more isolated winter polar vortex. Constituent concentrations in the southern hemisphere high-latitude stratosphere are therefore different from those in the northern hemisphere during the same season. As a result, the model southern hemisphere responds differently to increases in chlorine loading than the model northern hemisphere, as seen in Figure 2b.

It is well known that the dynamical behavior of the real southern hemisphere stratosphere is also different from the northern hemisphere [e.g., *Schoeberl and Hartmann*, 1991]. This difference between the behavior of the northern and southern hemispheres may result in conditions that produce an asymmetry in the O_3 trend in the real atmosphere.

In this paper, we diagnose the specific conditions in the interactive model that produce its asymmetric O_3 trend. We show that the model behavior is consistent with our theoretical expectations. Following this, we examine UARS data to see if the features causing the model trend asymmetry are apparent in the real atmosphere. Qualitative agreement between the model and the atmosphere will suggest that atmospheric mechanisms similar to those in the model may be producing the observed asymmetry in the SBUV trend calculation.

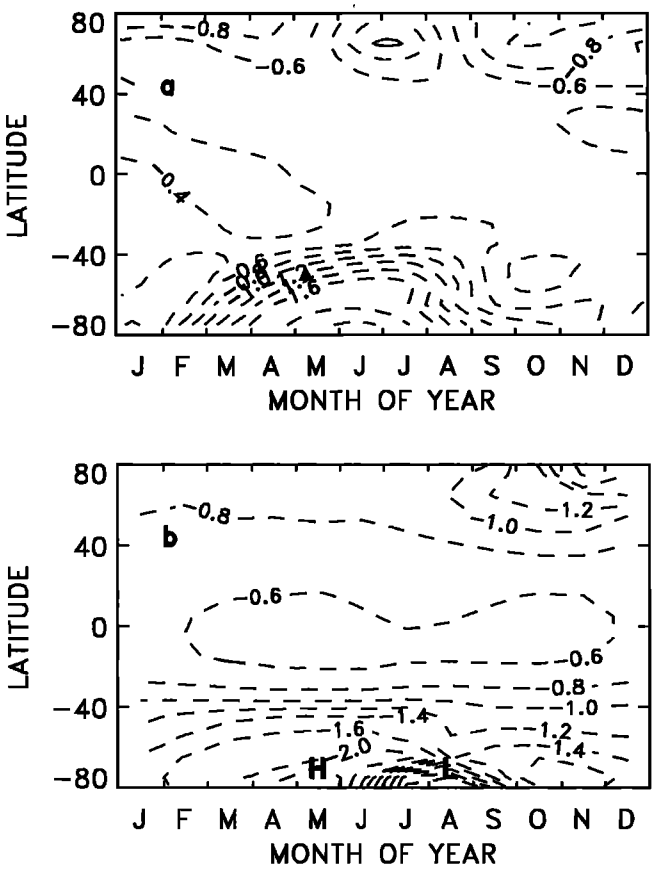

Figure 3. (a) Seasonal trends in O_3 in percent per year, calculated from the SBUV and SBUV 2 data set. Shown is an average of the 0.5-1 mbar and the 1-2 mbar layers. (b) Seasonal trends in O_3 calculated by the Goddard Space Flight Center interactive model. The 3 mbar layer trend is shown.

The remainder of this paper is devoted to this model analysis and its subsequent application to UARS observations. In section 2 we outline a theoretical approach to understanding the possible sources of interhemispheric asymmetries in the middle to upper stratospheric O_3 trend and support the theory with model output. Following this, various UARS data are examined for behavior similar to that found in the interactive model. A summary and some conclusions are provided in section 4.

2. Model Analysis

Figure 3a plots the seasonal trend coefficients from the combined SBUV and SBUV 2 data set in percent per year for the average of 0.5-1 mbar and the 1-2 mbar layers, as a function of the week of year and latitude. The interhemispheric trend asymmetry is more apparent in Figure 3a than the annually averaged trends plotted in Figure 1. The maximum trend magnitude in the southern hemisphere is more than 2 %/yr and occurs in late fall and early winter at high latitudes. The trend magnitude decreases to a minimum of about 0.4 %/yr in the late summer. In the northern hemisphere a maximum trend magnitude of just over 1 %/yr occurs in the fall. The minimum trend magnitude occurs in the summer as in the southern hemisphere, just reaching the zero trend mark in the 60 ° to 70° latitude band at week 26. As with the annually averaged trend asymmetry shown in Figure 1a, the differences between the southern and northern hemispheres are significant at the 1σ level.

Qualitatively similar behavior is seen in the interactive model. Figure 3b shows the seasonal trend plot from the interactive model at 3 mbar. The 3 mbar level is examined for several reasons. First, the northern hemisphere trend peaks at this level. Second, although it is not the model level with the largest trend asymmetry, the asymmetry that does exist at 3 mbar is still substantial. Third, there is only a small trend asymmetry in the model at the 1 mbar level where the observed trend asymmetry peaks. Fourth, the SBUV data have a relatively low resolution and do not precisely locate the peak trend asymmetry in altitude. The SAGE II instrument has significantly higher resolution and shows a peak trend occurring around 2 mbar. Our strategy is therefore to examine the 3 mbar model results and take the differences between the 3 mbar and 1 mbar levels into account when comparing the model results with observations.

The maximum trend magnitude at the 3 mbar level occurs in the southern hemisphere autumn with a peak magnitude of about 3 %/yr marked in Figure 3b by an "H." A rapid decrease in trend magnitude occurs over the course of the winter, with a minimum of about 0.1 %/yr marked in Figure 3b by "L," occurring in late winter at the highest latitudes. The trend magnitude then increases to a secondary maximum of over 1.5 %/yr in the spring. The northern hemisphere seasonal trend in the interactive model is very similar to the south-

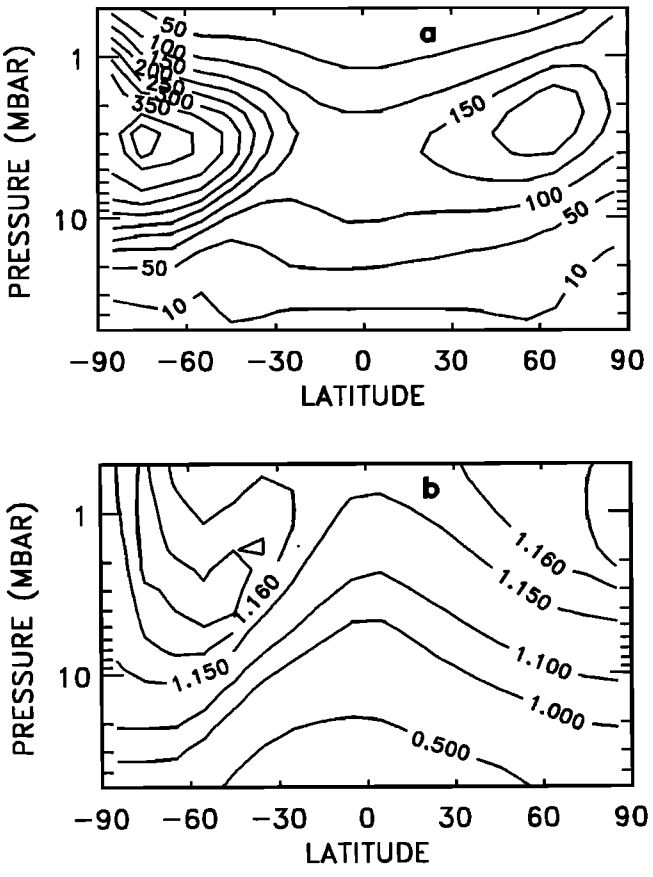

Figure 4. The 1980 to 1990 change in annually averaged ClO and Cl_y in the interactive model showing increases in (a) ClO in parts per trillion by volume and (b) increases in Cl_y in parts per billion by volume.

ern hemisphere, phase shifted by 6 months and with smaller magnitudes. The maximum trend in the northern hemisphere occurs in fall, with a secondary maximum in the spring. Although there are some differences between the SBUV-calculated trends and the model trends, the similarities between the two suggest that similar mechanisms may be responsible for the interhemispheric asymmetries in both the observations and the model calculation.

The interactive model O_3 trend is caused by increases in Cl_y. Figures 4a and 4b are plots of annually averaged difference in ClO and Cl_y between 1980 steady state and 1990 steady state interactive model runs, respectively. These figures show that the increase in model Cl_y is relatively symmetric and the increase in ClO is asymmetric. Comparison of the interactive model annually averaged O_3 trend in Figure 2b and the increase in ClO in Figure 4a shows that there is a strong correlation between the two. We therefore want to understand the relationship between the asymmetric changes in O_3 and ClO as well as the conditions that produce an asymmetric ΔClO from a symmetric ΔCl_y.

Consider a region of the atmosphere in photochemical equilibrium, where transport is unimportant. In this case the concentration of O_3 (denoted $[O_3]$) will be determined by the ratio of its chemical production and loss terms P_{O_3} and L_{O_3}, where P_{O_3} is the rate of O_3 production in molecules per unit volume persecond and L_{O_3} is the loss frequency in units of 1 persecond. If P_{O_3} remains constant and L_{O_3} changes by ΔL_{O_3}, then the fractional change in O_3 will be approximately

$$\frac{\Delta[O_3]}{[O_3]} \approx -\frac{\Delta L_{O_3}}{L_{O_3}}. \quad (1)$$

The O_3 loss frequency can be broken into contributions from Cl_y and other loss terms:

$$\begin{aligned} L_{O_3} &= L_{\text{oth}} + L_{Cl_y} \\ &= L_{\text{oth}} + 2k_{ClO,O}\left(\frac{O}{O_3}\right)\left(\frac{ClO}{Cl_y}\right)[Cl_y]. \end{aligned} \quad (2)$$

In (2), $k_{ClO,O}$ is the rate of the $ClO+O \rightarrow Cl+O_2$ reaction. This is the rate-limiting step of the catalytic cycle controlling O_3 destruction due to Cl_y. We have also introduced the ratios O/O_3 and ClO/Cl_y which can be determined by photochemical equilibrium assumptions. L_{oth} includes the loss of O_3 due to Chapman chemistry and the catalytic O_3 loss cycles involving odd hydrogen, nitrogen, and bromine species. If we assume that L_{oth} remains constant as Cl_y increases, then the fractional change in O_3 loss frequency and the fractional change in O_3 resulting from the increase ΔCl_y in Cl_y will be

$$\begin{aligned} \frac{\Delta O_3}{O_3} &\approx -\frac{\Delta L_{O_3}}{L_{O_3}} \\ &= -\frac{2k_{ClO,O}\left(\frac{O}{O_3}\right)\left(\frac{ClO}{Cl_y}\right)\Delta[Cl_y]}{L_{O_3}}. \end{aligned} \quad (3)$$

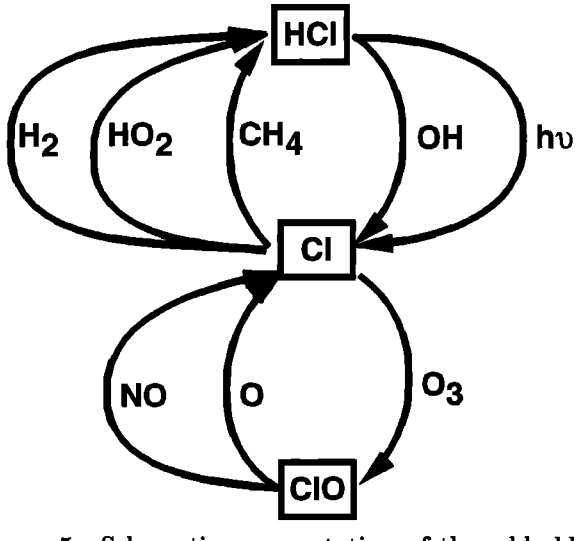

Figure 5. Schematic representation of the odd chlorine family at the 1 mbar level. Shown are the members, HCl, Cl, and ClO, and the reactions that are primarily responsible for establishing the partitioning of the family among its members. At this level, HOCl is predicted to be approximately 10% of Cl_y and so is neglected. The reaction $ClO + OH \rightarrow Cl + HO_2$ is also neglected because it is negligible at this altitude compared to $ClO + O \rightarrow Cl + O_2$.

Here we also assume that increases in Cl_y will not affect O_x or Cl_y partitioning.

Now consider a parcel in the southern hemisphere and a similar parcel in the northern hemisphere, both of which experience the same increase in Cl_y. If there is an interhemispheric asymmetry in the partitioning of Cl_y such that $(ClO/Cl_y)^{SH} = A(ClO/Cl_y)^{NH}$, then the northern hemisphere fractional change in O_3 loss frequency will be

$$\left(\frac{\Delta L_{O_3}}{L_{O_3}}\right)^{NH} = \frac{\Delta L_{Cl_y}^{NH}}{L_{oth} + L_{Cl_y}^{NH}}. \quad (4)$$

Assuming that the only difference between the northern and southern hemispheres is the Cl_y partitioning, the fractional change in O_3 loss frequency in the southern hemisphere will be

$$\left(\frac{\Delta L_{O_3}}{L_{O_3}}\right)^{SH} = \frac{A\Delta L_{Cl_y}^{NH}}{L_{oth} + AL_{Cl_y}^{NH}}. \quad (5)$$

Equations (4) and (5) show that the magnitude of the O_3 trend is determined by the size of $\Delta L_{Cl_y}^{NH}$ in relation to $L_{oth} + L_{Cl_y}^{NH}$, while the trend asymmetry is determined by the relative magnitudes of L_{oth} and $L_{Cl_y}^{NH}$. In the interactive model the fraction of Cl_y-catalyzed O_3 loss at high latitudes in the fall, where the O_3 trend is largest, ranges from about 40% of the total chemical loss at 3 mbar to about 70% at 1 mbar. Therefore one expects an asymmetry in the O_3 trend that is about half of the asymmetry in the Cl_y partitioning.

We now consider the factors controlling the Cl_y partitioning in the middle to upper stratosphere. Figure 5 shows schematically the principal members of the Cl_y family in this region and the primary reactions that result in the interconversion of the members into each other. At this altitude, Cl_y is mostly in the form of ClO and HCl, so $Cl_y \approx HCl + ClO$. Therefore

$$\frac{ClO}{Cl_y} \approx \frac{1}{1 + \frac{HCl}{ClO}}. \quad (6)$$

The key ratio in Cl_y partitioning in the upper stratosphere is therefore HCl/ClO. From the reactions shown in Figure 5, in photochemical equilibrium this ratio can be expressed as

$$\frac{HCl}{ClO} = \left(\frac{HCl}{Cl}\right)\left(\frac{Cl}{ClO}\right), \quad (7)$$

where

$$\frac{HCl}{Cl} = \frac{k_{Cl,CH_4}[CH_4] + k_{Cl,H_2}[H_2] + k_{Cl,HO_2}[HO_2]}{k_{HCl,OH}[OH] + j_{HCl}}, \quad (8)$$

$$\frac{Cl}{ClO} = \frac{k_{ClO,NO}[NO] + k_{ClO,O}[O]}{k_{Cl,O_3}[O_3]}. \quad (9)$$

Any asymmetry in the HCl/ClO ratio will be the result of asymmetries in the concentrations of the constituents in Equations (8) and (9) or temperature. These two equations therefore provide a list of possible sources of interhemispheric asymmetry in the O_3 trend. We can examine model output to determine the largest sources of its interhemispheric trend asymmetry which can then be compared with observations obtained by UARS.

Figure 6 shows the annual cycle for seven constituents, temperature, and the HCl photolysis coefficient from the 1990 steady state run of the interactive model as a function of month at 3 mbar. The solid line plots the values at 65°S, and the dashed line plots the corresponding northern hemisphere values, phase shifted by 6 months. The phase shift allows direct comparison of the northern and southern hemisphere annual cycles. We choose 65° because it is the highest model latitude that does not enter polar night where the above analysis would not apply. Of these species, OH, O, HO_2, and J_{HCl} display no significant interhemispheric asymmetry. Figure 6 shows that significant asymmetries in CH_4, NO, O_3, and H_2 that would affect Cl_y partitioning do occur. Values of CH_4, H_2, and NO in the southern hemisphere are lower than the northern hemisphere values which favor larger ClO concentrations in the southern hemisphere. The lower southern hemisphere O_3 values occurring during the winter months favor smaller concentrations of ClO. Finally, although northern hemisphere temperatures exceed southern hemisphere temperatures only by a maximum of 3%, the temperature sensitivity of the $Cl + CH_4 \rightarrow HCl + CH_3$ and $Cl + H_2 \rightarrow HCl + H$ reactions results in rates in the northern hemisphere that are up to 18% and 32% larger than the southern hemisphere wintertime values, respectively. The asymmetry in these reaction rates would favor larger values of ClO in the southern hemisphere.

The effect of the constituent asymmetries shown in Figure 6 on model ClO can be seen in Figure 7a whichshows the northern and southern hemisphere ClO concentrations at the 3 mbar model level, again at 65°S and 65°N. Plotted in Figure 7b is Cl_y, showing that the asymmetry in ClO seen in Figure 7a is not due to an asymmetry in inorganic chlorine concentrations.

The respective roles of the reactions shown in Figure 5 can be evaluated by determining the fraction of the total rate of conversion of one Cl_y member into another contributed by each reaction. This fraction will vary over the course of the year, so the reactions will be more important at some times and less important at others. For instance, Figure 5 shows that $Cl + CH_4 \rightarrow HCl + CH_3$ competes with $Cl + HO_2 \rightarrow HCl + O_2$ and $Cl + H_2 \rightarrow HCl + H$. The fraction of the total rate of conversion of Cl to HCl by the reaction of Cl and CH_4 is thus

$$f_{Cl,CH_4} = \frac{k_{Cl,CH_4}[CH_4]}{k_{Cl,CH_4}[CH_4] + k_{Cl,HO_2}[HO_2] + k_{Cl,H_2}[H_2]}. \quad (10)$$

Similar equations apply for the other reactions governing the partitioning of Cl_y at this altitude. Figures 8a and 8b show the interconversion fractions for four of the

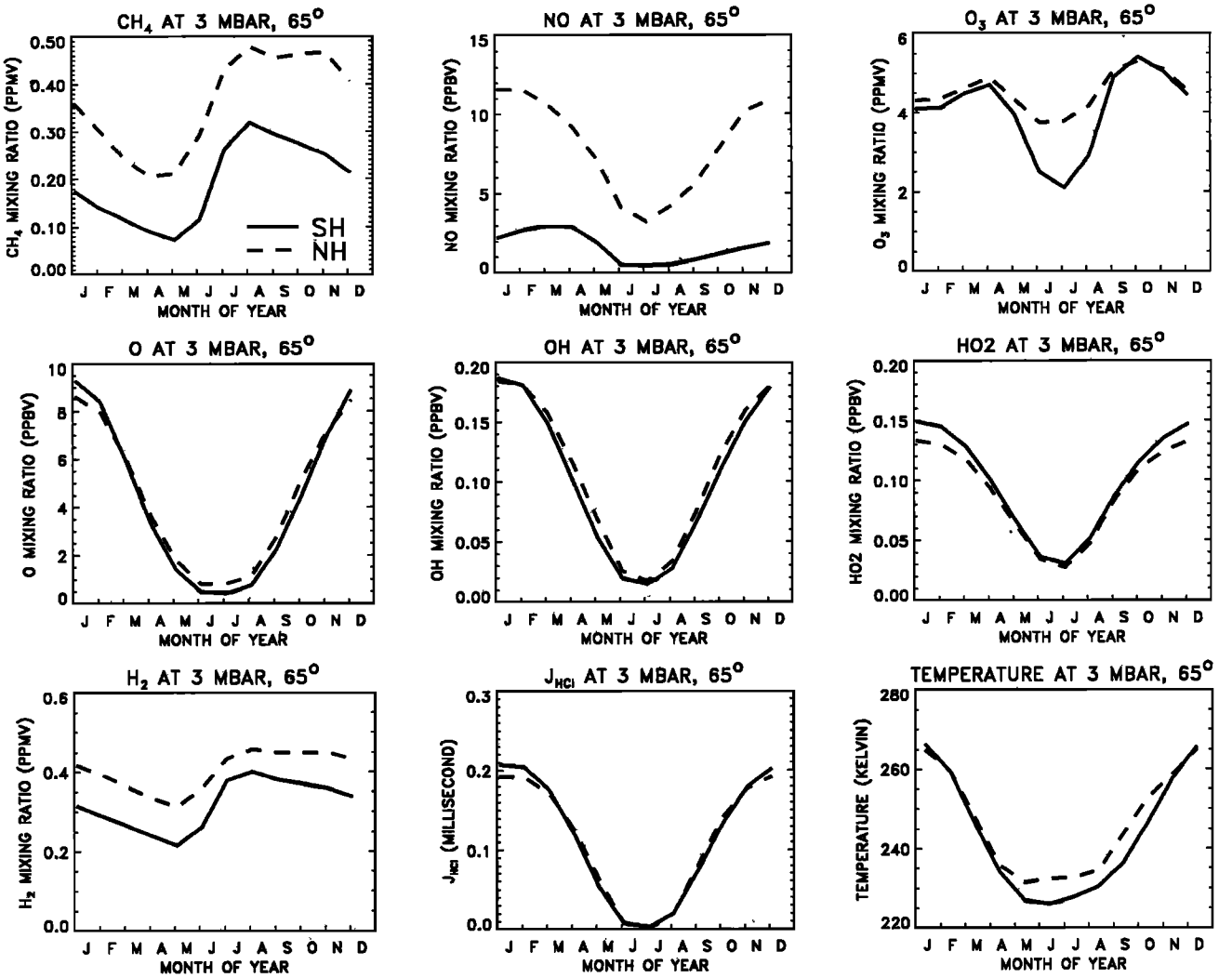

Figure 6. Seasonal dependence of a number of constituents, the HCl photolysis coefficient, and the model-calculated temperature at 3 mbar in the interactive model. The solid line denotes southern hemisphere values at 65°S. The dashed line denotes northern hemisphere values, phase shifted by 6 months to coincide with the southern hemisphere points.

reactions involved in Cl_y partitioning as a function of season at the 3 mbar level in the southern hemisphere. Figure 8 shows that the $Cl+CH_4 \rightarrow HCl+CH_3$ reaction is responsible for about 35% to 70% of the conversion of Cl to HCl, with the $Cl + HO_2 \rightarrow HCl + O_2$ reaction responsible for most of the rest. Figure 6 shows that while there is a substantial asymmetry in CH_4, the asymmetry in HO_2 is insignificant. The competition between the two reactions therefore reduces the impact of the asymmetry in CH_4 in the partitioning of Cl_y. Figure 8b shows an even larger dilution of the impact of the NO asymmetry on the Cl_y partitioning. This is because most of the conversion of ClO to Cl at the 3 mbar level is governed by $ClO + O \rightarrow Cl + O_2$, and O is not significantly asymmetric. It is interesting to note that at 1 mbar where the O_3 trend in the atmosphere observed by the SBUV instrument is largest, O concentrations are predicted by the model to be about a factor of 20 larger than they are at 3 mbar. Thus the role played in the partitioning of Cl_y by the ClO + NO reaction at 1 mbar is negligible.

The analysis presented above is based on the assumption that the primary reactions involved in Cl_y partitioning are shown in Figure 5. This is true for the model, but may not be true in the atmosphere. Atmospheric models using standard photochemical reactions tend to overestimate the amount of ClO in the 1 to 5 mbar region of the atmosphere compared with observations [*Chandra et al.*, 1993; *Dessler et al.*, 1996]. One suggestion that has been made to rectify the situation is to include a branching ratio for the reaction of ClO with OH to produce HCl [*McElroy and Salawitch*, 1989]. The normal product of the ClO + OH reaction is Cl, but a branching ratio to HCl of up to 14% cannot be ruled out by current laboratory measurements of this reaction rate [*DeMore et al.*, 1994]. If a 6% branching ratio to HCl is included, f_{Cl,CH_4} drops by between 12% (summer) and 47% (winter) near 1 mbar. This

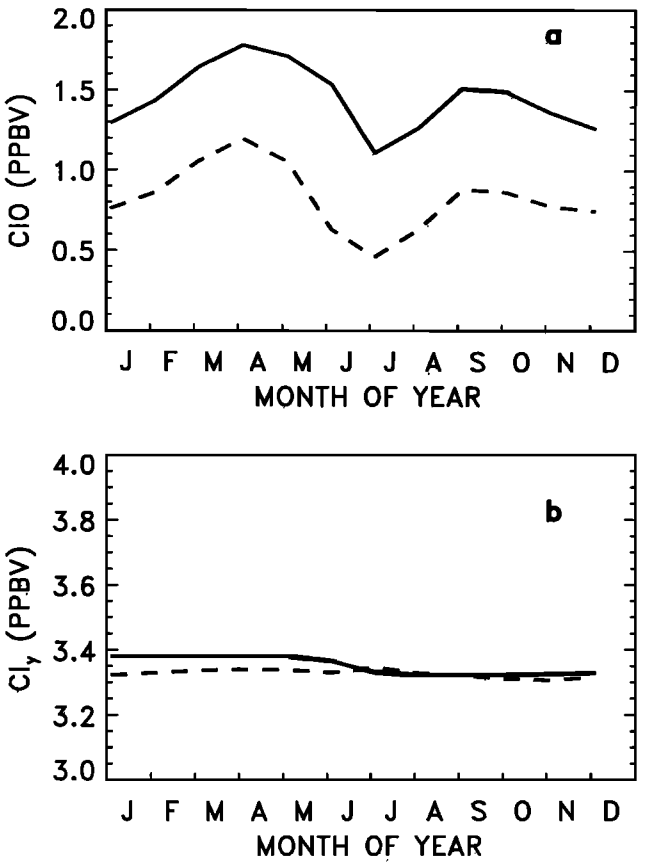

Figure 7. Seasonal dependence of (a) ClO and (b) Cl_y at 3 mbar in the interactive model. The solid line denotes southern hemisphere values at 65°S. The dashed line denotes 65°N northern hemisphere values, phase-shifted by six months to coincide with the southern hemisphere points.

could substantially reduce the effect of interhemispheric asymmetries in CH_4 on Cl_y partitioning.

3. UARS Data Analysis

The model analysis of section 2 provides a picture of how an O_3 trend asymmetry arises in the GSFC interactive two-dimensional (2D) model. Asymmetric forcing of the model circulation produces asymmetric long-lived tracer distributions. The asymmetries in the tracers result in an asymmetry in the model chlorine partitioning. Therefore symmetric increases in Cl_y result in asymmetric increases in ClO and asymmetric decreases in O_3. In the model, asymmetries in CH_4 and NO are the largest sources of model trend asymmetry. The UARS data set provides an opportunity to look for similar behavior in the atmosphere. In this section the available data are presented and compared with the results of section 2.

UARS measures several constituents that should be asymmetric if atmospheric mechanisms similar to those seen in the model results described above are producing the asymmetry seen in the SBUV data. First are the long-lived tracers CH_4 and N_2O. Because they are long-lived, these constituents are good indicators of dynamical processes in the atmosphere. CH_4 measurements are available from the improved stratospheric and mesospheric sounder (ISAMS), the halogen occultation experiment (HALOE), and cryogen limb array etalon spectrometer (CLAES). The most appropriate data set for this study is from CLAES because it samples high latitudes at the appropriate times of year and spans over a year of observations. The ISAMS instrument provides 180 days of observations [*Remedios et al.*, 1996], and the HALOE instrument does not observe high enough latitudes during the fall and winter [*Park et al.*, 1996]. The altitude range of CLAES CH_4 extends up to about 0.2 mbar, while the N_2O data are meaningful up to 1 mbar [*Roche et al.*, 1996].

As was shown in the section 2, a second major contributor to the interhemispheric asymmetry in model Cl_y partitioning is NO. As discussed above, at 1 mbar the rate of the $ClO + O \rightarrow Cl + O_2$ reaction is much larger than that of $ClO + NO \rightarrow Cl + NO_2$. Atmospheric asymmetries in NO are therefore not expected to play a role where the atmospheric trend asymmetries occur. This is fortunate because validated NO observations appropriate for this study are not currently available in the UARS data set.

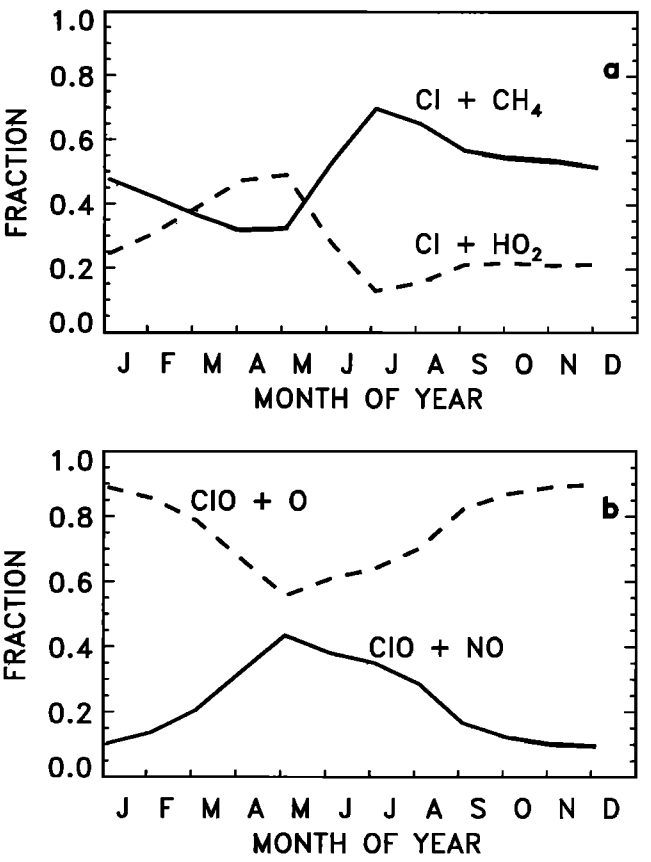

Figure 8. Conversion fractions for various reactions controlling Cl_y partitioning at 3 mbar and 65°S (see text for definition of conversion fraction.) a. Conversion fractions for the reactions $Cl + CH_4$ (solid line) and $Cl + HO_2$ (dashed line). b. Conversion fractions for the reactions $ClO + NO$ (solid line) and $ClO + O$ (dashed line).

The microwave limb sounder (MLS) provides observations of ClO, O_3, and temperature. Although O_3 and temperature were not major contributors to the asymmetries seen in the model data, they could play a role in the atmosphere. Unlike the CLAES data that are available only through April 1993, the MLS data set extends to the present. These constituents will be examined to the extent that the data set allows below.

In the following data analysis we chose to look at the latitude band between 65° and 70° for the CLAES data and the 60° to 70° band for the MLS data and to follow the changes in the various constituent concentrations over the course of the year. There are several reasons for this choice. First, the O_3 trend asymmetry seen in the SBUV data is a function of latitude and pressure, suggesting that we should intercompare the hemispheres at the same latitude and pressure level. Second, because the trend and the trend asymmetry are largest at high latitudes, the data analysis should consider higher latitudes. Third, the mechanism we are investigating as the potential source of the trend asymmetry is one that requires sunlight. At latitudes higher than 60° to 70° there are too few daylight observations to obtain robust yaw cycle averages from the relatively imprecise MLS ClO observations.

Because we are constructing zonal mean averages at high latitudes in fall and winter, the averages include data taken both inside and outside the polar vortex. To check possible influences of the vortex on our results, we used potential vorticity and the potential vorticity gradient to construct zonal mean averages using only observations from inside the vortex and compared them with the averages including all the observations. We found no differences large enough to affect the conclusions of the data analysis. Apparently, the altitudes of interest here are above the region where the polar winter vortex is a strong barrier to horizontal transport, so the region inside the vortex is not as chemically distinct as it is at lower altitudes where the isolation is stronger [e.g., *Schoeberl and Hartmann*, 1991].

3.1. CLAES CH_4 and N_2O

Figure 9a compares the annual cycle of CH_4 in the northern and southern hemispheres in 1992 at 1 mbar using CLAES version 7 data. Each point represents the zonal mean of all the data retrieved between 65° and 70° for an entire yaw cycle. The northern hemisphere data have been phase shifted by 6 months so that the southern and southern hemisphere annual cycles can be compared directly. The crosses in Figure 9 are southern hemisphere points, and the asterisks are northern hemisphere values. Error bars on the points represent the precision of the data and do not include estimates of accuracy uncertainty. Accuracy uncertainties would shift both northern and southern hemisphere observations away from their true values in a similar manner. The accuracy of the observations is therefore irrelevant in this interhemispheric comparison. The error bars are generally smaller than the data points for these averages.

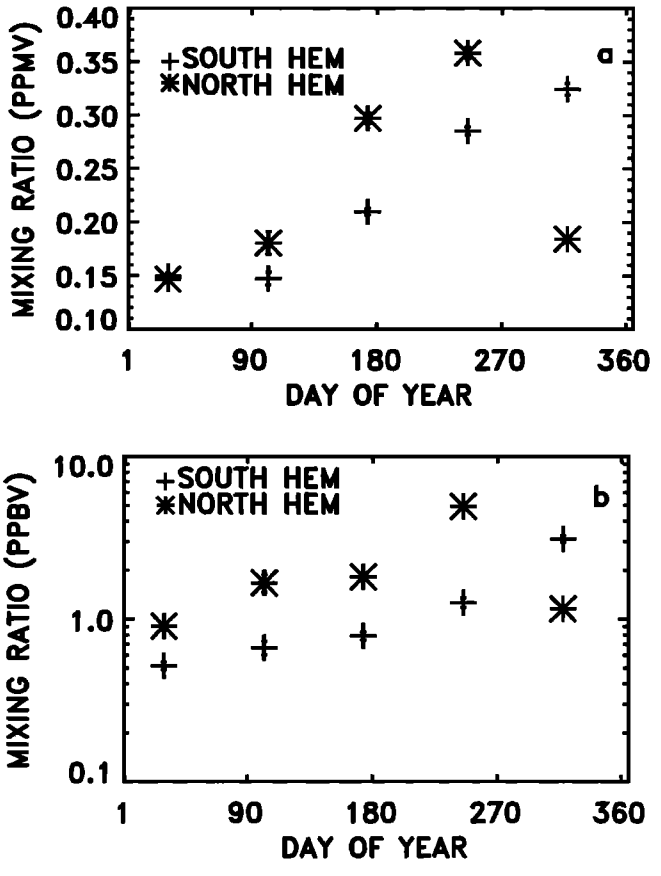

Figure 9. Seasonal behavior of version 7 cryogenic limb array etalon spectrometer (CLAES) (a) CH_4 and (b) N_2O in 1992 for the northern and southern hemispheres. Each point is an average over all retrieved values not flagged as bad data for an entire yaw cycle at the 1 mbar level, between 65° and 70° latitude. Units are parts per million by volume for CH_4 and parts per billion by volume for N_2O. Crosses represent values for the southern hemisphere and asterisks represent northern hemisphere values. Error bars representing the standard error of the data are drawn but sometimes the standard error is smaller than the plotting symbol. The northern hemisphere values have been phase shifted by 6 months so the northern hemisphere and southern hemisphere points coincide on the plots.

In both hemispheres, CH_4 values are similar and near their annual minimum at the end of the summer at this altitude. During the fall in both hemispheres, CH_4 increases rapidly, with values in the northern hemisphere somewhat larger than those in the southern hemisphere. During the winter and spring, CH_4 continues to increase in both hemispheres, though the rate of increase slows compared to the fall. Northern hemisphere CH_4 values are 20% to 50% larger than southern hemisphere during these two seasons. At the end of spring and the beginning of summer, in November in the southern hemisphere and and May in the northern hemisphere, a reversal occurs such that southern hemisphere CH_4 is about twice as large as in the northern hemisphere. It appears that CH_4 in the northern hemisphere begins to

relax back to the low values characteristic of the late summer earlier than what occurs in the southern hemisphere.

Analogous behavior is seen in version 7 CLAES N_2O, shown in Figure 9b. Note that the data are plotted on a semilogarithmic scale. Unlike CH_4, N_2O is not directly involved in determining Cl_y partitioning. However, the observed asymmetry in CLAES N_2O corroborates the CH_4 observations. A minimum in N_2O occurs sometime in the late summer. The fall and winter values in the northern hemisphere at high latitudes average about a factor of 2 larger at this altitude than in the southern hemisphere, emphasizing that a distinct asymmetry exists between these two regions in 1992 which lowers long-lived tracer mixing ratios in the southern hemisphere compared with the northern hemisphere.

The latitudinal behavior of CH_4 and N_2O during the winter of 1992 is shown in Figures 10a and 10b at the 1 mbar level. Each point is a zonal mean average over 5° latitude bands for the June/July 1992 yaw cycle in the southern hemisphere and the December 1992/January 1993 yaw cycle in the northern hemisphere. The plots show that the southern hemisphere winter values are significantly lower than the northern hemisphere values over a range of higher latitudes.

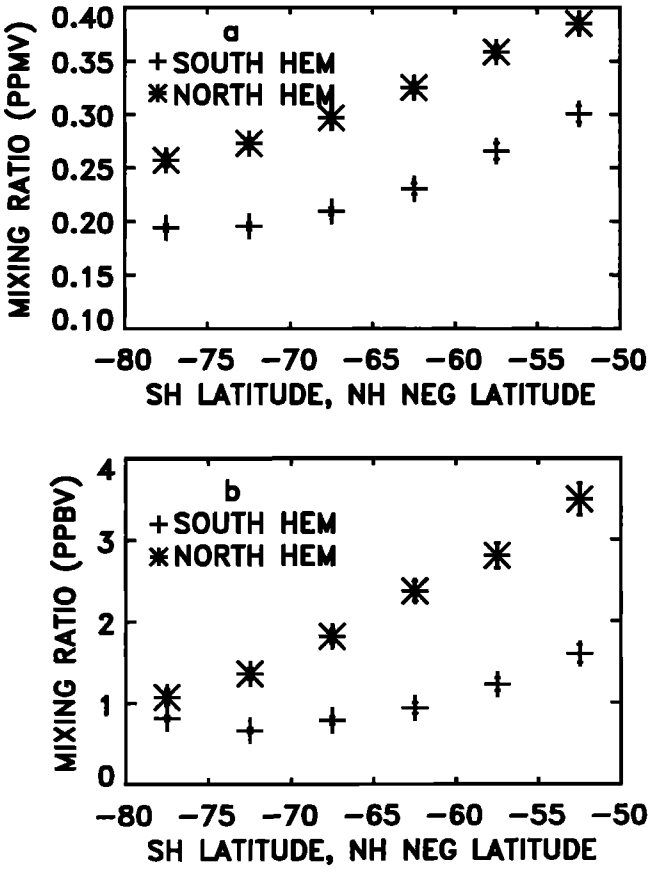

Figure 10. Same as Figure 9, but for latitudinal behavior. The northern hemisphere values are plotted as a function of negative latitude so that the northern hemisphere and southern hemisphere points coincide on the plots.

While the SBUV trends in the southern hemisphere shown in Figure 1a peak at around 1 mbar, in the SAGE II trend analysis of *Wang et al.* [1996] the peak trend occurs at around 2 mbar. In addition, peak values of ClO from MLS also occur around 2 mbar. It is therefore interesting to know how the asymmetry in CH_4 and N_2O changes with altitude. Both CH_4 and N_2O in the 65° to 70° latitude band maintain lower values in the southern hemisphere than the northern hemisphere, down to about 10 mbar. Northern hemisphere N_2O is consistently about a factor of 2 larger than the corresponding southern hemisphere values. The asymmetry between southern and northern hemisphere CH_4 does not appear to be quite as strong at lower altitudes, with northern hemisphere values around 25% larger than the southern hemisphere values in contrast to the 50% differences which occur in the 1 mbar region.

The difference between the southern and northern hemispheres seen in the CLAES data is not as great as the difference between the southern and northern hemisphere high latitudes in the interactive model. For instance, Figure 6 shows that northern hemisphere CH_4 in the interactive model during June and July at 65° and 3 mbar is about a factor of 2 larger than the southern hemisphere value. The CLAES data shown in Figure 10a differ by about 50% between the southern and northern hemispheres. Although this is less than seen in the interactive model, the CLAES CH_4 observations show that in 1992 a situation existed that would favor higher ClO levels at high latitudes in the southern hemisphere. If the behavior of the atmosphere in 1992 is typical, then one would expect persistently higher values of ClO to occur in the southern rather than the northern hemisphere.

3.2. MLS O_3 and Temperature

O_3 plays an important role in the partitioning of Cl_y, as can be seen in the schematic representation of the Cl_y family in Figure 5 and (9). In the model results shown in Figure 6, O_3 displays no interhemispheric asymmetry during the fall. In the late winter, northern hemisphere O_3 values are up to 50% higher than those in the southern hemisphere, promoting ClO over HCl in the northern hemisphere. This asymmetry is one reason that the late winter/early spring model O_3 trends seen in Figure 3b are smaller than those occurring in the late fall.

The annual cycle of O_3 as observed by MLS at 1 mbar is shown in Figure 11a, which was made using version 4 data averaged between 60° and 70° in the northern and southern hemispheres. As in previous plots, each of the values shown in Figure 11a is an average over an entire yaw cycle. Summertime values are quite similar in the northern and southern hemispheres, with values of about 2.3 ppmv. During the fall, O_3 concentrations nearly double in both hemispheres, with O_3 in the southern hemisphere about 8% higher than the northern hemisphere. No asymmetry between the hemispheres exists in the winter, but a difference of about 25% occurs in the spring, with northern hemisphere lev-

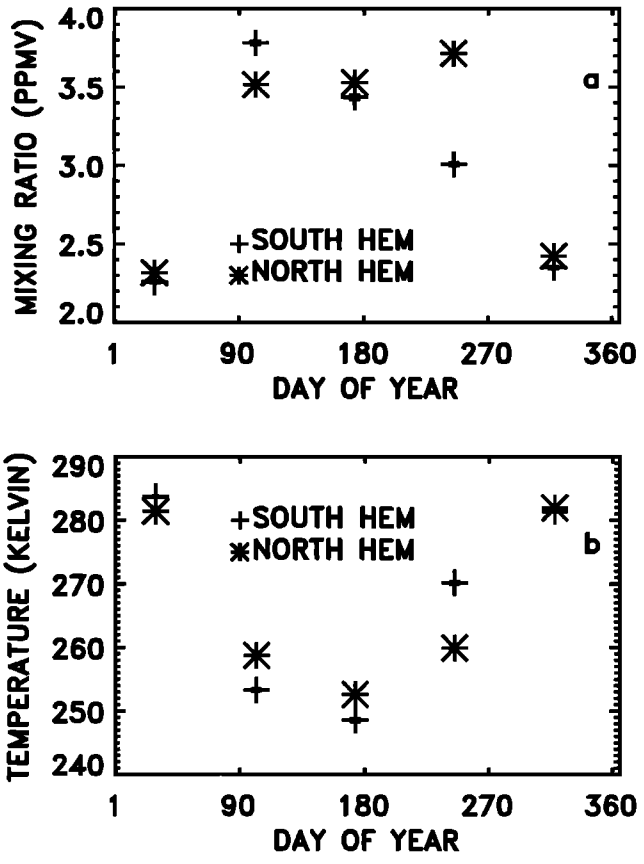

Figure 11. Seasonal behavior of version 4 microwave limb sounder (MLS) (a) O_3 and (b) temperature in 1992 for the northern and southern hemispheres. Each point is an average over all retrieved values not flagged as bad data for an entire yaw cycle at the 1 mbar level, between 60° and 70° in latitude. Values are in parts per million by volume for O_3 and Kelvin for temperature. Crosses represent values for the southern hemisphere and asterisks represent northern hemisphere values. Error bars representing the standard error of the data are drawn, but sometimes the standard error is smaller than the plotting symbol. The northern hemisphere values have been phase shifted by six months so the northern hemisphere and southern hemisphere points coincide on the plot.

els higher than those in the southern hemisphere. The O_3 concentrations observed by the MLS instrument in 1992 would not result in large fall and winter interhemispheric differences in Cl_y partitioning at high latitudes in the 1 mbar region.

The annual cycle of temperature as observed by MLS in 1992 at 1 mbar averaged between 60° and 70° in the northern and southern hemispheres is shown in Figure 11b. In both the northern and southern hemispheres the temperature peaks in the summer and has a minimum in the winter. At no time are there any asymmetries that exceed 10%. However, the southern hemisphere appears to warm up more rapidly in spring, and the maximum differences between the two hemispheres at this altitude and latitude occur at that time.

In the winter of 1992 the southern hemisphere is colder than the northern hemisphere by about 1.6%. This temperature asymmetry would favor somewhat larger values of ClO in the southern hemisphere than the northern hemisphere.

3.3. MLS ClO

The UARS constituent asymmetries examined above would produce an asymmetry in the O_3 trend by affecting Cl_y partitioning to favor ClO. The MLS instrument on UARS has been observing ClO since its launch in September 1991, so several years of ClO observations are available for examination. The ClO data are useful up to 1 mbar [*Waters et al.*, 1996]. Plotted in Figures 12a-12c are the seasonal cycles of daytime average ClO from version 4 data at 1 mbar for 1992, 1993, and 1994, respectively. The points represent averages of all the daytime data available for each yaw cycle observed between 60° and 70° in the northern and southern hemispheres. Figure 12 shows that peak values of ClO tend to occur in the fall and winter, when O_3 trends are largest. However, southern hemisphere ClO values are not consistently larger than the northern hemisphere values, as would be expected if the trend asymmetry were due to interhemispheric differences in Cl_y partitioning.

In 1992 we can combine model output with observations of CLAES CH_4 and MLS O_3 and temperature to predict an approximate asymmetry between southern and northern hemisphere ClO from (8) and (9). In the fall of 1992 at 1 mbar between 65° and 70° latitude, southern hemisphere ClO is predicted to be about 7% larger than northern hemisphere ClO. In the winter, southern hemisphere ClO is predicted to be about 25% larger than the northern hemisphere values. Most of this asymmetry is caused by the asymmetry in CH_4, with O_3 and temperature playing similar, smaller roles. This predicted asymmetry in ClO is too small to account for the trends calculated from the SBUV observations. Given the uncertainty in the ClO data, it is not possible to determine whether the predictions derived from (8) and (9) are consistent with the observed ClO.

Figure 12 shows that large asymmetries in southern and northern hemisphere ClO concentrations did not occur in 1992, 1993, or 1994. Output from the interactive model suggests that factor of 2 differences between southern and northern hemisphere ClO during the fall or winter maintained over the SBUV and SBUV 2 observing period would be required to produce the observed asymmetries in the O_3 trend. Such differences should be observable in the MLS ClO data averaged over a yaw cycle. Thus, if the observed asymmetries in the O_3 trend are due to asymmetries in Cl_y partitioning, other years besides 1992, 1993, or 1994 would have to be responsible for the trend.

4. Summary and Conclusions

Trends in O_3 in the 1 to 3 mbar region calculated from SBUV observations are significantly more negative in

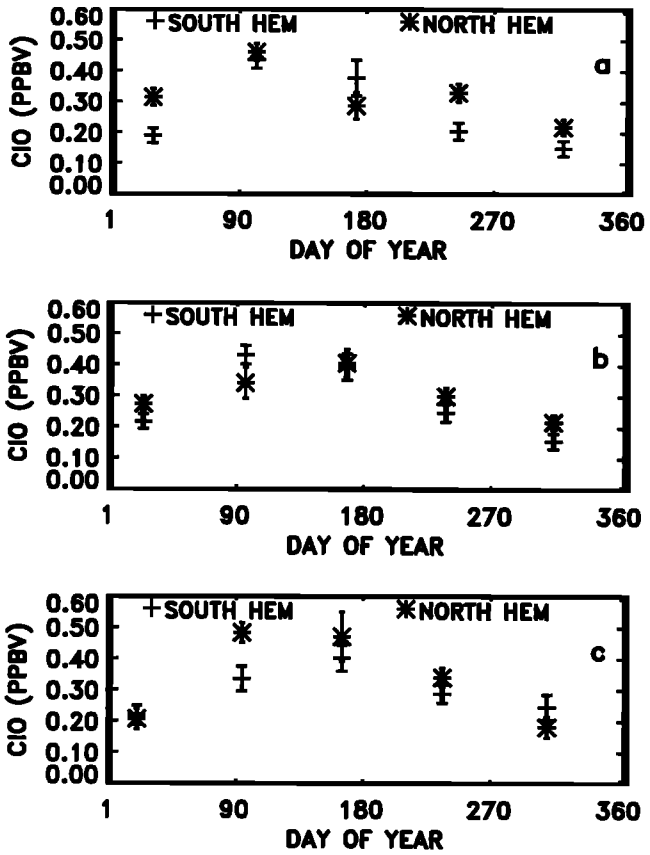

Figure 12. Seasonal behavior of version 4 MLS daytime ClO in (a) 1992, (b) 1993, and (c) 1994 for the northern and southern hemispheres. Each point is an average over all daytime retrieved values not flagged as bad data for an entire yaw cycle at the 1 mbar level, between 60° and 70° in latitude. Values are given in parts per billion by volume. Crosses represent values for the southern hemisphere and asterisks represent northern hemisphere values. Error bars representing the standard error of the data are drawn, but sometimes the standard error is smaller than the plotting symbol. Error bars for the southern hemisphere points have wider crossbars to distinguish them from northern hemisphere error bars. The northern hemisphere values have been phase shifted by 6 months so the northern hemisphere and southern hemisphere points coincide on the plot.

the southern compared with the northern hemisphere. A recent calculation of O_3 trends using SAGE data exhibits a similar asymmetry. To date, no mechanism that might explain the asymmetry has been proposed.

Trends in O_3 calculated using the GSFC 2D interactive model are asymmetric and qualitatively similar to the SBUV trends, unlike other models that have been used in profile O_3 trend calculations. The model trend is due to large dynamical differences between the northern and southern hemispheres, particularly in the fall and winter. These dynamical differences result in lower values of CH_4 and NO in the southern hemisphere high latitudes than in the northern hemisphere. Since these constituents play an important role in Cl_y partitioning, their asymmetry creates large interhemispheric differences in the partitioning of Cl_y. Much more of the southern hemisphere Cl_y at high latitudes is in the form of ClO than that at northern hemisphere high latitudes. When Cl_y is added to the model by the breakdown of increased amounts of chlorofluorocarbons, the southern hemisphere increase in ClO is larger than in the northern hemisphere. The larger increase in ClO in the southern hemisphere results in larger O_3 destruction and a larger O_3 trend.

To determine whether a similar mechanism might be responsible for the asymmetric atmospheric trend calculated from SBUV and SBUV 2 satellite observations, we examined various data from UARS. Atmospheric observations of CH_4 and N_2O from the CLAES instrument in 1992 are lower in the southern hemisphere fall and winter than in the northern hemisphere. This suggests that there are dynamical asymmetries between the northern and southern hemispheres in the atmosphere that are similar to those in the model. In addition, given our current understanding of photochemistry in the high-latitude 1 mbar region, the lower observed values of CH_4 in the southern hemisphere are consistent with a Cl_y partitioning that would favor ClO. However, the asymmetry in ClO that we calculate should be produced by the observed asymmetry in CH_4 in 1992 would not be large enough to produce the observed O_3 trend asymmetry.

Observations of O_3 and temperature from the MLS instrument show small asymmetries between the northern and southern hemisphere that should not produce large differences in Cl_y partitioning between the two hemispheres.

Observations of ClO in 1992, 1993, and 1994 by the MLS are not significantly different in the northern as opposed to the southern hemispheres. In 1992 the precision of the ClO observations is not sufficient to determine if there is an asymmetry consistent with that expected from the CH_4, O_3, and temperature observations. However, the precision of the ClO data is good enough to show that the 50% to factor of 2 differences between the southern and northern hemispheres needed to explain the SBUV trend asymmetries did not occur in 1992, 1993, or 1994. If the observed interhemispheric differences in ClO for these years are typical of all the years in the SBUV data set, then the mechanism producing the observed atmospheric trend asymmetry could not be the same as the model trend asymmetry mechanism.

Other mechanisms that might explain the O_3 trend asymmetry include asymmetric transport of O_3 out of the high-latitude upper stratosphere and asymmetries in temperature. This can be seen by examining (4) and (5) in the model analysis. We assumed that the O_3 loss due to sources other than Cl_y, L_{oth}, was the same in both hemispheres. If instead $L_{oth}^{SH} < L_{oth}^{NH}$, then a symmetric increase in Cl_y-catalyzed loss would result in a larger southern hemisphere trend. The L_{oth} term includes the loss of O_3 due to transport, Chapman chemistry, HO_x, and NO_x. At high latitudes at the 1

mbar level, O_3 loss due to the very temperature sensitive Chapman $O + O_3 \rightarrow 2O_2$ reaction is the largest chemical loss process after Cl_y-catalyzed O_3 loss. Investigating these possibilities is a subject for further research.

The UARS data provide evidence of an asymmetry in long-lived tracer concentrations between the northern and southern hemisphere in the high-latitude, 1 mbar region. In the GSFC interactive model a similar tracer asymmetry produces interhemispheric photochemical differences that result in an asymmetric O_3 trend. In the UARS data we have examined, we find no evidence of a similar photochemical situation which would explain an asymmetric O_3 trend if maintained over a number of years. This does not imply that a mechanism similar to the model mechanism does not occur in the atmosphere. Other, unobserved years may be responsible for the atmospheric trend. However, it is impossible to determine whether or not this is the case due to a lack of observations in these years. If ClO observations are continued in the future, a deeper understanding of the interannual behavior of this constituent in the high-latitude, 1 mbar region could arise, which would indicate whether the model mechanism also operates in the Earth's atmosphere.

Acknowledgments. The authors would like to thank Stacey Hollandsworth for providing calculations of the O_3 trend obtained from SBUV and SBUV 2 satellite data and Anne R. Douglass for helpful discussions. A. E. Dessler was supported by a postdoctoral fellowship granted by the National Research Council while this research was being conducted.

References

Bacmeister, J. T., M. R. Schoeberl, M. E. Summers, J. R. Rosenfield, and X. Zhu, Descent of long-lived trace gases in the winter polar vortex, *J. Geophys. Res., 100*, 11,669-11,684, 1995.

Chandra, S., C. H. Jackman, A. R. Douglass, E. L. Fleming, and D. B. Considine, Chlorine catalyzed destruction of ozone: Implications for ozone variability in the upper stratosphere, *Geophys. Res. Lett., 20*, 351-354, 1993.

Considine, D. B., A. R. Douglass, and C. H. Jackman, Effects of a parameterization of nitric acid trihydrate cloud formation on 2D model predictions of stratospheric ozone depletion due to stratospheric aircraft, *J. Geophys. Res., 99*, 18,879-18,894, 1994.

DeMore, W. B., D. M. Golden, R. F. Hampson, C. J. Howard, C. E. Kolb, M. J. Kurylo, M. J. Molina, A. R. Ravishankara, and S. P. Sander, Chemical kinetics and photochemical data for use in stratospheric modeling, evaluation Number 11, *JPL Publication 94-26*, 1994.

Dessler, A. E., S. R. Kawa, D. B. Considine, J. W. Waters, L. Froidevaux, and J. B. Kumer, UARS measurements of ClO and NO_2 at 40 and 46 km and implications for the 'Ozone Deficit', *Geophys. Res. Lett., 23*, 339-342, 1996.

Douglass, A. R., C. H. Jackman, and R. S. Stolarski, Comparison of model results transporting the odd nitrogen family with results transporting separate odd nitrogen species, *J. Geophys. Res., 94*, 9862-9872, 1989.

Hollandsworth, S. M., R. D. McPeters, L. E. Flynn, W. Planet, A. J. Miller, and S. Chandra, Ozone trends deduced from combined Nimbus 7 SBUV and NOAA 11 SBUV 2 data, *Geophys. Res. Lett., 22*, 905-908, 1995.

Hood, L. L., R. D. McPeters, J. P. McCormack, L. E. Flynn, S. M. Hollandsworth, and J. F. Gleason, Altitude dependence of stratospheric ozone trends based on Nimbus 7 SBUV data, *Geophys. Res. Lett., 20*, 2667-2670, 1993.

Jackman, C. H., A. R. Douglass, R. B. Rood, R. D. McPeters, and P. E. Meade, Effect of solar proton events on the middle atmosphere during the past two solar cycles as computed using a two-dimensional model, *J. Geophys. Res., 95*, 7414-7428, 1990.

McElroy, M. B., and R. J. Salawitch, Changing composition of the global stratosphere, *Science, 243*, 763-770, 1989.

Park, J. H., et al., Validation of halogen occultation experiment CH_4 measurements from the UARS, *J. Geophys. Res., 101*, 10,183-10,203, 1996.

Remedios, J. J., et al., Measurements of methane and nitrous oxide distributions by the improved stratospheric and mesospheric sounder: Retrieval and validation, *J. Geophys. Res., 101*, 9843-9872, 1996.

Roche, A. E., et al., Validation of CH_4 and N_2O measurements by the cryogenic limb array etalon spectrometer instrument on the Upper Atmosphere Research Satellite, *J. Geophys. Res., 101*, 9679-9710, 1996.

Rosenfield, J. E., D. B. Considine, P. E. Meade, J. T. Bacmeister, C. H. Jackman, and M. R. Schoeberl, Stratospheric effects of Mount Pinatubo aerosol studied with a coupled two-dimensional model, *J. Geophys. Res., 102*, 3649-3670, 1997.

Schoeberl, M. R., and D. L. Hartmann, The dynamics of the stratospheric polar vortex and its relation to springtime ozone depletions, *Science, 251*, 46-52, 1991.

Wang, H. J., D. M. Cunnold, and X. Bao, A critical analysis of Stratospheric Aerosol and Gas Experiment ozone trends, *J. Geophys. Res., 101*, 12,495-12,514, 1996.

Waters, J. W., et al., Validation of UARS microwave limb sounder ClO measurements, *J. Geophys. Res., 101*, 10,091-10,128, 1996.

World Meteorological Organization (WMO), Scientific assessment of stratospheric ozone: 1989, *Rep. 20*, Global Ozone Res. and Monit. Proj., World Meteorol. Org., Geneva, 1990.

World Meteorological Organization (WMO), Scientific assessment of stratospheric ozone: 1994, *Rep. 37*, Global Ozone Res. and Monit. Proj., World Meteorol. Org., Geneva, 1995.

D. B. Considine and A. E. Dessler, Joint Center for Earth System Science, Department of Meteorology University of Maryland, College Park, MD, 20742. (email: dbc@welkin.gsfc.nasa.gov)

C. H. Jackman, P. E. Meade, J. E. Rosenfield, and M. R. Schoeberl, NASA Goddard Space Flight Center, Code 916, Greenbelt, MD, 20771.

A. E. Roche, Lockheed Palo Alto Research Laboratories, Org 91-20/Building 252, 3251 Hanover Street, Palo Alto, CA, 94304.

J. W. Waters, NASA Jet Propulsion Laboratory, Mail Code 183-701, 4800 Oak Grove Drive, Pasadena, CA, 91109.

(Received November 22, 1996; revised August 7, 1997; accepted August 13, 1997.)